Journal of the Serbian Chemical Society
JSCS-info@shd.org.rs • www.shd.org.rs/JSCS
J. Serb. Chem. Soc. *86* (4) 393–406 (2021)
JSCS–5429
Original scientific paper

Structural study of Pt(II) and Pd(II) complexes with quinoline-2-carboxaldehyde thiosemicarbazone

PREDRAG G. RISTIĆ[1], MARKO V. RODIĆ[2#], NENAD R. FILIPOVIĆ[3#], DRAGANA M. MITIĆ[4#], KATARINA K. ANĐELKOVIĆ[1#] and TAMARA R. TODOROVIĆ[1]*

[1]*University of Belgrade – Faculty of Chemistry, Studentski trg 12–16, 11000 Belgrade, Serbia,* [2]*Faculty of Sciences, University of Novi Sad, Trg Dositeja Obradovića 3, 21000 Novi Sad, Serbia,* [3]*University of Belgrade – Faculty of Agriculture, Nemanjina 6, 11000 Belgrade, Serbia and* [4]*Innovation Centre of Faculty of Chemistry, University of Belgrade, Studentski trg 12–16, 11000 Belgrade, Serbia*

(Received 26 November, revised 1 December, accepted 2 December 2020)

Abstract: Two square–planar complexes, [PtLCl] (**1**) and [PdLCl] (**2**), were synthesized with quinoline-2-carboxaldehyde thiosemicarbazone ligand (HL), and characterized by IR and NMR spectroscopy and single crystal X-ray diffraction analysis. In both complexes, L^- is coordinated tridentately *via* the same donor atom set, while the fourth coordination site is occupied by a chloride ion. However, the complexes are not isostructural due to different types of non-covalent intermolecular interactions. These interactions were analyzed using Hirshfeld surfaces and two-dimensional fingerprint plots.

Keywords: single crystal X-ray diffraction; non-covalent interactions; *N*-heteroaromatic Schiff base; chelate complexes.

INTRODUCTION

During the last decades, thiosemicarbazones have been developed as organic compounds with very diverse pharmacological applications. They show a broad range of biological activity, such as antituberculosis, antiviral, antimalarial and anticancer.[1,2] It is assumed that the strong metal-chelating/-interacting properties of thiosemicarbazones and their interference with the cellular iron and copper homeostasis play an important role in their biological activity.[1]

Thiosemicarbazones are well known ligands that coordinate to various metal ions in different modes. In general, a bidentate binding mode *via* N,S donor atom set is the most common one.[3,4] However, the chelating capacity of thiosemicarbazones can be enhanced when additional suitable donor atoms are present in the

* Corresponding author. E-mail: tamarat@chem.bg.ac.rs
# Serbian Chemical Society member.
https://doi.org/10.2298/JSC201126079R

molecule, as in the case of *α*-*N*-heterocyclic thiosemicarbazones.[3,4] As thiosemicarbazones exist as thione–thiol tautomers, they can bind to a metal center in the neutral or anionic forms. An overview on the observed bonding modes for this class of ligands is given in several reviews in literature covering this field.[3–5]

Thiosemicarbazone complexes have shown potent biological activity, such as anticancer, antibacterial, antifungal, and antiviral, owing to their property to diffuse through the semi permeable membrane of cell lines.[2,4–6] The enhanced effect of the complexes in comparison to free ligands may be attributed to their increased lipophilicity. Namely, upon coordination to the metal ion, the ligand orient with the lipophilic and aromatic parts outwards, exposing the hydrophobic part to the exterior.[3] This allows the complex to enter the cell and could explain the reason why complexes are more active than the parent ligands.

One line of previous research was focused on the synthesis, characterization and biological activity evaluation of d-metal complexes with *α*-*N*-heterocyclic chalcogensemicarbazones, predominantly derivatives of 2-formylpyridine and quinoline-2-carboxaldehyde.[7–14] Taking into account that many properties of chemical systems are defined not only by the molecular structure but also by weak intermolecular interactions,[15,16] herein the synthesis and characterization of Pd(II) and Pt(II) complexes with quinoline-2-carboxaldehyde thiosemicarbazone, with the main focus on the solid state structures and main interactions that govern the crystal packing, are reported. Both chosen ions have a d^8 electronic configuration and almost the same ionic radii; thus, their complexes with the same ligand systems are often isostructural. However, the higher basicity of the 5d Pt(II) ion and its extended electronic density in comparison to the 4d Pd(II) ion can often result in stronger M···H−X (X = C, N, O, S) interactions for Pt(II).[17] These effects can lead to a difference in the molecular structure and especially packing features of the complexes.[18]

EXPERIMENTAL

Materials and methods

Thiosemicarbazide (97 %), and quinolone-2-carboxaldehyde (97 %) were obtained from Acros Organics (BVBA, Geel, Belgium), while potassium tetrachloroplatinate(II) (98 %), and potassium tetrachloropalladate(II) (98 %) were obtained from Aldrich (Sigma–Aldrich). All solvents (reagent grade) were obtained from commercial suppliers and used without further purification.

Elemental analyses (C, H, N, S) were performed by the standard micromethods using an Elementar Vario ELIII C,H,N,S/O analyzer, and the results were found to be in good agreement (±0.4 %) with the calculated values. The IR spectra were recorded on a Thermo Scientific Nicolet 6700 FT-IR spectrophotometer by the attenuated total reflection (ATR) technique in the region 4000–400 cm^{-1}. Abbreviations used for IR spectra: *vs*, very strong; *s*, strong; *m*, medium; *w*, weak; *vw*, very weak. Molar conductivities were measured at room temperature (298 K) on the Crison multimeter MM41. The NMR spectra were obtained on a Bruker Avance 500 instrument equipped with a broadband direct probe. All spectra were measured at

298 K in DMSO-d_6. Chemical shifts are given on the δ scale (ppm) relative to tetramethylsilane (TMS) as the internal standard for ^{1}H and ^{13}C.

Synthesis of quinoline-2-carboxaldehyde thiosemicarbazone (HL)

The ligand was synthesized, as described previously[19] in the condensation reaction of quinoline-2-carboxaldehyde (0.862 g, 5.5 mmol) and thiosemisemicarbazide (0.500 g, 5.5 mmol) in ethanol (EtOH, 50 mL). The purity of the ligand was checked by elemental analysis and NMR spectroscopy.

Synthesis of quinoline-2-carboxaldehyde thiosemicarbazonato-N,N,S-*chloridoplatinum(II), [PtLCl] (**1**)*

Into a suspension of HL (0.100 g, 0.44 mmol) in EtOH (10 mL), a solution of $K_2[PtCl_4]$ (0.180 g, 0.43 mmol) in 1 mL of water was added. The reaction mixture was refluxed for 1 h. After cooling to room temperature, the obtained dark red microcrystals were separated by filtration and washed with cold EtOH. Single crystals of **1** suitable for X-ray diffraction analysis were obtained by slow diffusion of EtOH vapor into DMSO solution of microcrystals. Single crystals of **1** were separated by filtration and washed with cold EtOH.

Synthesis of quinoline-2-carboxaldehyde thiosemicarbazonato-N,N,S-*chloridopalladium(II), [PdLCl] (**2**)*

Into a suspension of HL (0.050 g, 0.22 mmol) in EtOH (10 mL), a solution of $K_2[PdCl_4]$ (0.068 g, 0.21 mmol) in 1 mL of water was added. The reaction mixture was refluxed for 1 h. After cooling to room temperature, the obtained orange microcrystals were separated by filtration and washed with cold EtOH. Single crystals of **2** suitable for X-ray diffraction analysis were obtained by slow diffusion of EtOH vapor into a DMSO solution of microcrystals. Single crystals of **2** were separated by filtration and washed with cold EtOH.

IR and NMR spectral data and spectra of HL, **1** and **2** are given in Figs. S-1–S-9 of the Supplementary material to this paper.

X-Ray crystallography

Diffraction data were collected on a Gemini S diffractometer (Oxford Diffraction), equipped with a Mo$K\alpha$ radiation source (λ = 0.71073 Å) and a Sapphire CCD detector. Data collection strategy calculation and data reduction were performed with CrysAlisPro.[20] Structure was solved by SHELXT,[21] and refined with the SHELXL-2014.[22] The SHELXLE[23] was used as a graphical user interface for the refinement procedures. All non-hydrogen atoms were refined anisotropically. The hydrogen atoms attached to C atoms were placed at the geometrically idealized positions with C–H distances fixed to 0.93 and 0.96 Å for sp^2 and sp^3 C atoms, respectively. Their isotropic displacement parameters were set equal to 1.2 and 1.5 Ueq of the parent sp^2 and sp^3 C atoms, respectively. The hydrogen atoms attached to N atoms were located in a difference Fourier map and refined isotopically. The structures were validated with Platon[24] together with extensive use of Mercury CSD 2020.2.0[25,26] and the Cambridge Crystallographic Database (CSD).[27]

A summary of the crystallographic data for the crystal structures is given in Table I.

Hirshfeld surfaces and two-dimensional (2D) fingerprint plots

For visualization of the Hirshfeld surfaces, CIF files were used. Hirshfeld surface visualization, presentation of results as d_{norm}, shape index, and curvedness, and calculation of 2D fingerprint plots with d_e and d_i distances were generated using Crystal Explorer v.17.5.[28,29] The distance from the surface to the nearest nucleus of the atom on the outside of the surface is denoted as d_e, while the distance from the surface to the closest nucleus of the atom on the

inside of the surface is denoted as d_i. The surfaces are mapped over a standard color scale, and 2D fingerprint plots are calculated using d_e and d_i values in the range 0.4−2.8 Å.

TABLE I. Crystallographic data and refinement parameters for **1** and **2**

Compound	**1**	**2**
Chemical formula	$C_{11}H_9ClN_4PtS$	$C_{11}H_9ClN_4PdS$
M_r	459.82	371.13
Crystal system	Monoclinic	Triclinic
Space group	$P2_1/n$	$P\bar{1}$
a /Å	11.1555(3)	8.6723(8)
b / Å	7.1925(2)	8.7320(8)
c / Å	16.2149(5)	9.5468(9)
V / Å^3	1250.61	612.90
Z	4	2
D_x / Mg m^{-3}	2.442	2.011
Radiation type	Mo$K\alpha$ (λ = 0.71073 Å)	Mo$K\alpha$ (λ = 0.71073 Å)
μ / mm^{-1}	11.585	1.886
Crystal size, mm	0.75×0.11×0.06	0.42×0.16×0.05
	Data collection	
Absorption correction	Analytical	Analytical
T_{min}, T_{max}	0.059, 0.529	0.859, 0.969
Reflections collected	11576	4636
Independent reflections	2970	2749
Observed reflections [$I > 2\sigma(I)$]	2631	2463
R_{int}	0.065	0.022
Range of h, k, l	h=−14→15, k=−8→9, l=−22→18	h=−11→11, k=−11→11, l=−12→11
θ values, °	θ_{max} = 29.0, θ_{min} = 2.6	θ_{max} = 28.7, θ_{min} = 2.5
	Refinement	
$R[F^2 > 2\sigma(F^2)]$, wR	0.021, 0.043	0.028, 0.055
R[all data], wR	0.027, 0.045	0.034, 0.059
Goodness-of-fit (S)	1.078	1.064
No. of reflections	2970	2749
No. of parameters	171	171
No. of restraints	0	2
$\Delta\rho_{max}$, $\Delta\rho_{min}$ / e Å^{-3}	0.63, −0.97	0.40, −0.65
CCDC No.	2044686	2044685

RESULTS AND DISCUSSION

Synthesis and spectroscopic characterization

By direct reaction of $K_2[PtCl_4]$ or $K_2[PdCl_4]$ with the ligand HL in an equimolar ratio (1:1), the corresponding Pt(II) (**1**) and Pd(II) (**2**) complexes were obtained (Scheme 1). The mole ratio of the reacting species did not influence the composition of the products. The same products were also obtained by a template reaction of metal salts with quinoline-2-carboxaldehyde and thiosemicarbazide in an equimolar ratio (1:1:1). Both complexes are soluble at room temperature in

DMSO and DMF, but sparingly soluble at elevated temperature in EtOH. The synthesized complexes are non-electrolytes, as determined by molar conductivity measurements. Elemental analysis showed that the molecules of Pt(II) and Pd(II) complexes contain one deprotonated ligand molecule and a chloride ion. In the ^{1}H-NMR spectra of both complexes, the H–N3 proton signal (at 11.77 ppm in the ligand) is missing, indicating coordination of the ligand in the deprotonated form. The IR spectrum of the free ligand HL exhibits bands at 3393, 3265 and 3146 cm^{-1} arising from asymmetric and symmetric NH_2 stretching vibrations.[30] Coordination of azomethine nitrogen to the metal ions in both complexes is suggested by the shift of the ν(C=N) towards higher frequencies (1605 cm^{-1} in HL, 1632 cm^{-1} in **1**, 1638 cm^{-1} in **2**). As a consequence of the coordination of sulfur atom, the ν(C–S) band in the IR spectra of the complexes is shifted to lower frequencies (816 cm^{-1} in **1** and 817 cm^{-1} in **2**) with respect to the metal free ligand (840 cm^{-1}). In both complexes, coordination *via* the quinoline nitrogen atom can be assumed as ring stretching (1527, 1501 and 1451 cm^{-1}) and the in-plane (750 cm^{-1}) modes of the heterocyclic ring are shifted to higher frequencies.[30] The solid state structure of the complexes was elucidated by single crystal X-ray analysis (*vide infra*).

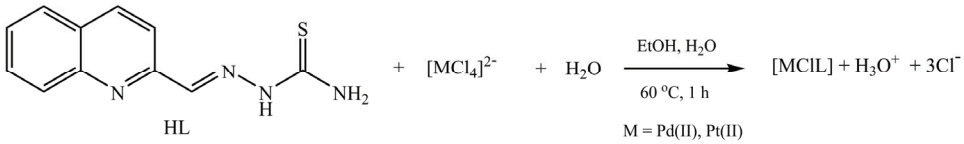

Scheme 1. Synthesis of Pt(II) and Pd(II) complexes.

*Molecular structures of **1** and **2***

Complexes **1** and **2** crystallize in the monoclinic $P2_1/n$ and triclinic $P\bar{1}$ space groups, respectively. The asymmetric unit of **1** and **2** contains the M(II) ion and one deprotonated ligand coordinated *via* sulfur atom, quinoline and imine nitrogen atoms (Fig. 1). The fourth coordination site is occupied by a chloride ligand. The overlay of the structures shows differences in the value of angles between the donor atoms of the ligand (Fig. 1). The coordination geometry around the metal centers is slightly distorted square–planar with geometric index of distortion $\tau = 0.10$ for **1** and $\tau = 0.13$ for **2**.[31] Due to the similar ionic radii of the metal ions, the lengths of coordination bonds (M–N1, M–N2, M–Cl and M–S) and corresponding bond angles are similar in both complexes (Table II).

As previously noticed for related thiosemicabazone complexes,[3–5] in **1** and **2** the C1–S1 bond is a much longer than a double bond while the adjacent C1–N3 bond is shorter than a single bond, indicating a prevalent thiolate resonance form of the coordinated ligand.

Although **1** and **2** have the same geometry, their crystal packings are different. With the exception of the nitrogen atoms, there are no classical proton donors, thus crystal packing in both complexes are based mainly on weak non-conventional interactions. An obvious limitation in the analysis of non-conventional contacts using the tools available in the CSD Mercury[25,26] is the application of distance criteria to determine the presence of a contact since interactions can extend beyond sums of van der Waals radii.[32,33] To gain further insights into the way molecules of **1** and **2** pack in their crystals, Hirshfeld surface analysis and noncovalent interaction plots (*vide infra*) were employed.

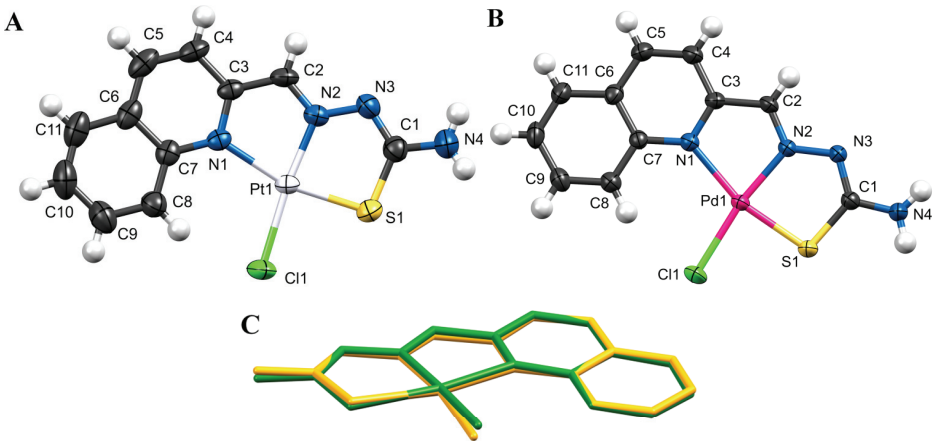

Fig. 1. Perspective view and labeling of molecular structure of **1** (A) and **2** (B). Thermal ellipsoids are shown at the 50 % probability level. Hydrogen atoms are shown as spheres of arbitrary radius. The overlay of the molecular structures of **1** (green) and **2** (yellow) (C).

TABLE II. Selected bond lengths and angles for **1** and **2**

Bond	Bond length, Å	Angle	Angle, °
Pt1–Cl1	2.3092(10)	N2–Pt1–N1	79.88(12)
Pt1–N1	2.125(3)	N2–Pt1–S1	84.93(10)
Pt1–N2	1.946(3)	N1–Pt1–Cl1	106.18(8)
Pt1–S1	2.2453(10)	S1–Pt1–Cl1	89.16(4)
Pd1–Cl1	2.3236(8)	N2–Pd1–N1	80.07(9)
Pd1–N1	2.149(2)	N2–Pd1–S1	84.18(7)
Pd1–N2	1.964(2)	N1–Pd1–Cl1	108.73(6)
Pd1–S1	2.2237(8)	S1–Pd1–Cl1	87.04(3)

Hirshfeld surface and 2D fingerprint plot analysis

The Hirshfeld surface and 2D fingerprint plot analysis represent important tools in exploring, understanding and describing crystal packing.[28,34] The Hirshfeld surfaces mapped over d_{norm} utilize the function of normalized distances d_i and d_e, where d_i and d_e are the distances from a given point on the surface to the

nearest atom inside and outside the surface, respectively. The long interatomic contacts, the contact at van der Waals separations and short interatomic contacts can be seen on the d_{norm}-mapped Hirshfeld surfaces as the blue, white and red color regions, respectively. Further chemical insight into the molecular packing can be obtained using curvedness and shape-index. Interactions can be observed in the shape-index plot as red and blue regions, as well as in the curvature plot as a flat zone in the same position of the surface as in the shape-index plot. On the shape index, red-colored regions correspond to an acceptor, while blue-colored regions belong to the donor of an intermolecular interaction.

2D Fingerprint plots, derived form a Hirshfeld surface, are a useful method to summarize complex information about intermolecular interactions in a crystal.[34] The color of each point on the plot, corresponding to the relative area of a (d_e, d_i) pair, is recognized as the contribution from different interatomic contacts: blue, green and red correspond to small, moderate and greatest contributions, respectively. An uncolored region indicates no contribution to the Hirshfeld surface.

The Hirshfeld surfaces of the complexes are depicted in Fig. 2, while the pseudosymmetric 2D fingerprint plots are depicted in Fig. 3.

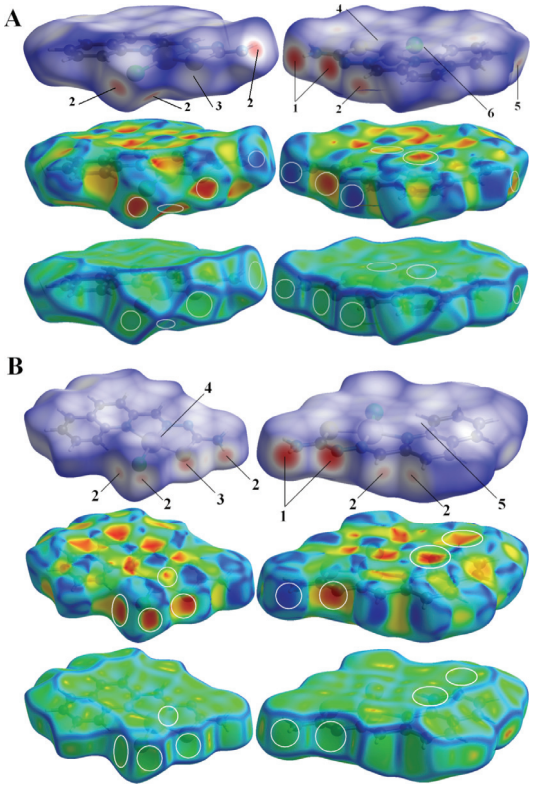

Fig. 2. Two views of the Hirshfeld surface mapped with d_{norm} (top), shape-index (middle) and curvedness (bottom), for **1** (A) and **2** (B). The numbers indicate points of contact derived from intermolecular interactions (see Table III).

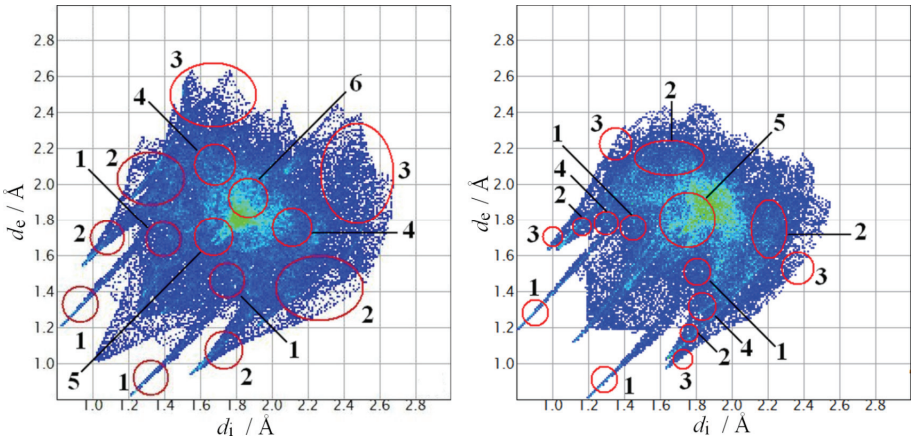

Fig. 3. Full 2D fingerprint plots for **1** (left) and **2** (right). For the interaction types see Table III.

TABLE III. Relative contributions and (d_i + d_e) of different interaction types in the crystal structures of **1** and **2**; M = Pt in **1**; M = Pd in **2**

No.	Interaction type	**1**		No.	**2**	
		Relative contribution %	(d_i +d_e) Å		Relative contribution %	(d_i +d_e) Å
1	N···H	8.6	2.0	1	9.8	2.0
2	Cl···H	16.5	2.6	2	16.8	2.7
3	S···H	11	3.1	3	8.7	2.6
4	M···H[a]	2.1	3.4	4	1.5	3.4
5	C···H	8.4	4.1	/	/	/
6	Cg···Cg	6.2	3.6	5	5.3	3.8

In the crystal structure of **1**, each molecule of the complex achieves six types of non-covalent intermolecular interactions/contacts, resulting in a three dimensional (3D) supramolecular structure. On the other hand, each molecule of **2** forms five types of intermolecular interactions. The relative percentage contributions of close contacts to the overall Hirshfeld surfaces in both crystal structures are presented in Table III.

The brightness of the red spots on the Hirshfeld surfaces mapped over d_{norm} can be qualitatively correlated with the strength of intermolecular contact, *i.e.*, as potential hydrogen bonds (bright spots), weak interactions (diminutive spots) or short (faint spots) interatomic contacts.[35] The bright-red spots indicated with '1' on the Hirshfeld surfaces mapped over d_{norm} (Fig. 2) indicate to donors and acceptors of classical hydrogen interactions involving N4 nitrogen atoms as donors and N3 nitrogen atoms as acceptors. The bright-red spots indicated with '2' on the same surfaces indicate the chlorine atom Cl1 as a double acceptor in both crystal structures. However, the corresponding donors are different. In **1**, the donors are N4 and C2 atoms, while in **2**, the donors are C2 and C4. The sulfur

atom S1 in **1** is involved in probable short interatomic contact with the C11 carbon atom, as can be seen from the faint spot indicated with '3'. In contrast, the sulfur atom S1 in **2** is an acceptor in the probable weak non-classical hydrogen bonding with the N4 nitrogen atom as donor, since the spot indicated with '3' is bright red. To examine π–π stacking in the molecular packing, an analysis of the Hirshfeld surface mapped over the shape-index and curvedness properties can be used (Fig. 2). The π–π stacking between the quinoline rings is indicated by the appearance of small blue regions surrounding bright-red spots within the rings (Fig. S-10 of the Supplementary material). The presence of these interactions is also evident as the flat regions around the rings on the Hirshfeld surface mapped over curvedness for both complexes.

The relative contributions of different types of intermolecular interactions in the crystal structures of **1** and **2** are different (Table III). This is a consequence of different symmetries of the space groups in which the complexes crystallize. The common feature for both complexes is that non-classical Cl···H interactions are most represented, probably because the chlorine atom is a double hydrogen bond acceptor. Finally, 2D fingerprint plots indicate the presence of M···H non-classical hydrogen interactions in both crystal structures (Fig. S-11 of the Supplementary material).

Analysis of crystal packing

The packing of molecules in the crystal structure of **1** is depicted in Fig. 4A. Each molecule of **1** forms a centrosymmetric dimer with a neighboring molecule *via* N4–H4B···N3^{i} (*i* = –*x*, 1–*y*, 1–*z*) hydrogen interaction (*D*···*A* = 3.039 Å, <N–H···N = 175.8°). A centrosymmetric dimer is also formed by C5–H5···Pt1^{ii} (*ii* = –1+*x*, –1+*y*, *z*) weak non-classical hydrogen interaction (*D*···*A* = 3.542 Å, <C–H···Pt = 89.9°). These two interactions are responsible for the formation of 1-D infinite chains parallel to the [110] direction (Fig. 4B). The coordinated Cl1 atom is a double acceptor involved in two non-classical hydrogen interactions, N4–H4A···Cl1^{iii} (*iii* = ½*x*, –1/2+*y*, 1.5–*z*; D···A = 3.385 Å, <N–H···Cl = 141.6°) and C2–H2···Cl1^{iv} (*iv* = –1/2+*x*, 1.5–*y*, –1/2+*z*; *D*···*A* = 3.527 Å, <C–H···Cl = 161.6°), as depicted in Fig. 4C. Sulfur atom S1 is involved in weak intermolecular contact C11–H11···S1^{v} (*v* = 1/2+*x*, 1.5–*y*, –1/2+*z*; *D*···*A* = 4.156 Å, <C–H···S = 159.7°; Fig. 4D). Finally, in the crystal packing of **1** there are π–π stacking interactions responsible for the formation of dimers (Fig. 4E) with a Cg···Cg^{vi} distance of 3.60 Å (*vi* = 1–*x*, 2–*y*, 1–*z*; Cg is the centre of gravity of the pyridine part of the ring).

The packing of molecules in the crystal structure of **2** is depicted in Fig. 5A. The same N4–H4B···N3^{i} (*i* = –*x*, 1–*y*, –*z*; *D*···*A* = 3.009 Å, N–H···N = 175.7°) interactions are responsible for the formation of centrosymmetric dimers. Each dimer unit is connected to a neighboring complex molecule by weak hydrogen

interactions involving the metal center (C11–H11···Pd1^{ii}, *ii* = 1–*x*, –*y*, 1–*z*; D···A = 3.369 Å, <C–H···Pd = 84.0°), thus forming a chain parallel to the [1–1 1] direction (Fig. 5B).

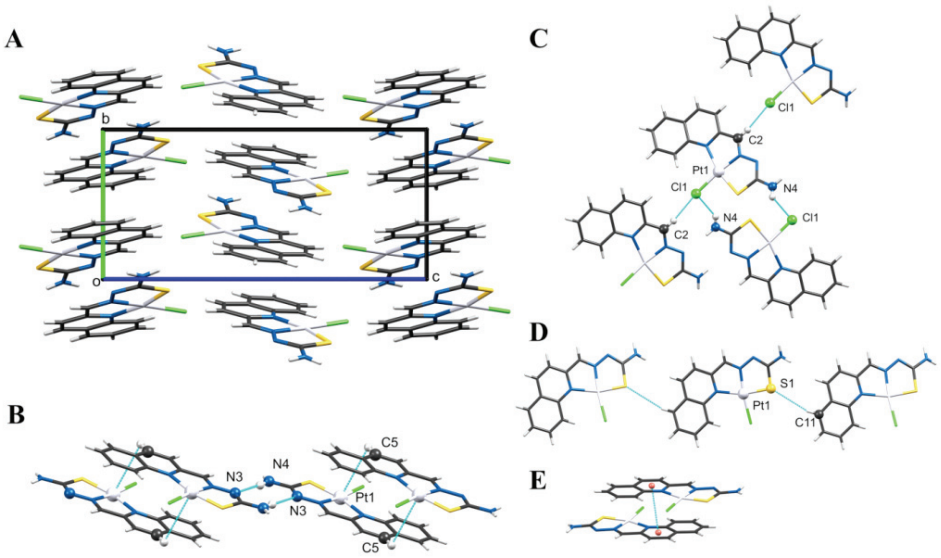

Fig. 4. Non-covalent interactions in the crystal packing of **1**. A) The packing of molecules in the crystal structure; B) a chain parallel to the [110] direction formed by C–H···Pt interactions; C) C–H···Cl and N–H···Cl interactions in the crystal structure of **1**; D) C–H···S contacts in the crystal structure of **1**; (E) π–π stacking interactions.

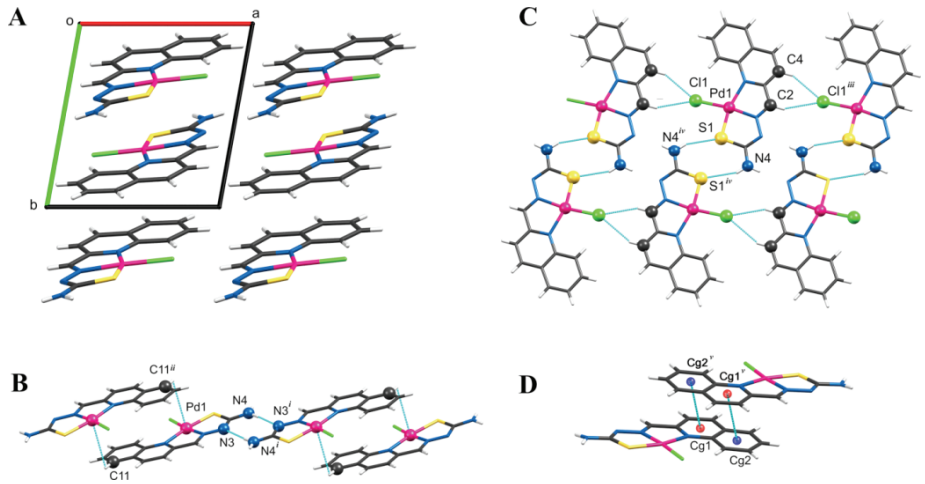

Fig. 5. Non-covalent interactions in the crystal packing of **2**. A) The packing of molecules in the crystal structure; B) a chain parallel to the [1–1 1] direction formed by C–H···Pd interactions; C) 2D plane, parallel to (021), formed by C–H···Cl and N–H···S interactions in the crystal structure of **2**; D) π–π stacking interactions.

Although the Cl1 atom is also a double acceptor in weak hydrogen interactions, as in **1**, these interactions involve carbon atoms C2 and C4 (C2–H2···Cl1^{iii}, *iii* = –1 + *x*, *y*, *z*; *D*···*A* = 3.636 Å, <C–H···Cl = 150.4° and C4–H4···Cl1^{iii}, D···A = = 3.653 Å, <C–H···Cl = 153.3°), thus a 1D infinite chain parallel to *a*-axis is formed. This chain is further connected by weak interactions involving the S1 atom from an adjacent complex molecule (N4–HA···S^{iv}, *iv* = 1–*x*, 1–*y*, –*z*; D···A = 3.542 Å, <N–H···S = 156.2°) thus a 2D plane parallel to (021) is formed (Fig. 5C). There are also π–π stacking interactions responsible for the formation of dimers (Fig. 5D) with a Cg1···Cg2^{v} distance of 3.76 Å (*v* = 1–*x*, –*y*, 1–*z*; Cg1 and Cg2 are the centre of gravity of the pyridine part and benzene part of the quinoline ring, respectively).

CONCLUSION

Herein, the synthesis, spectroscopic characterization and single crystal X-ray diffraction analysis of novel square–planar Pt(II) and Pd(II) complexes with quinoline-2-carboxaldehyde thiosemicarbazone are presented. In both complexes, the ligand is tridentately coordinated in the anionic form *via* the sulfur, quinoline and imine nitrogen donor atoms. The fourth coordination site is occupied by a chlorido ligand. Despite the similar ionic radii of the metal ions and respective coordination bond lengths, crystal packing of the complexes is different. Detailed analysis of non-covalent interactions revealed that non-classical Cl···H interactions are the most represented in both crystal structures. The coordinated chlorine atom is involved in bifurcated non-classical hydrogen interactions. In both crystal structures, one interaction involves the imine carbon atom as a donor. However, in the second interaction, the thioamide nitrogen atom is a donor in the case of **1**, while in the crystal packing of **2**, the interaction involves the *meta* carbon atom of the pyridine part of the aromatic ring. This might contribute to the difference in crystal packings of the synthesized complexes.

SUPPLEMENTARY MATERIAL

Additional data are available electronically at the pages of journal website: https://www.shd-pub.org.rs/index.php/JSCS/index, or from the corresponding author on request.

Additional crystallographic data for the structures reported in this paper have been deposited at the Cambridge Crystallographic Data Centre with quotation numbers CCDC 2044685 and 2044686. They are available free of charge on request *via* www.ccdc.cam.ac.uk/data_request/cif

Acknowledgement. This work was financially supported by the Ministry of Education, Science and Technological Development of the Republic of Serbia (Contract No: 451-03-68/2020-14/200168).

И З В О Д

СТРУКТУРНА СТУДИЈА КОМПЛЕКСА Pt(II) И Pd(II) СА ХИНОЛИН-2-КАРБОКСАЛЕДЕХИД ТИОСЕМИКАРБАЗОНОМ

ПРЕДРАГ Г. РИСТИЋ[1], МАРКО В. РОДИЋ[2], НЕНАД Р. ФИЛИПОВИЋ[3], ДРАГАНА М. МИТИЋ[4], КАТАРИНА К. АНЂЕЛКОВИЋ[1] и ТАМАРА Р. ТОДОРОВИЋ[1]

[1]Универзитет у Београду – Хемијски факултет, Студентски трг 12–16, 11000 Београд, [2]Природно–математички факултет, Универзитет у Новом Саду, Трг Доситеја Обрадовића 4, 21000 Нови Сад, [3]Универзитет у Београду – Пољопривредни факултет, Немањина 6, 11000 Београд и [4]Иновациони центар Хемијског факултета, Универзитет у Београду, Студентски трг 12–16, 11000 Београд

Синтетисана су два квадратно–планарна комплекса, [PtLCl] (**1**) и [PdLCl] (**2**), са хинолин-2-карбоксалдехид тиосемикарбазонским лигандом (HL), који су окарактерисани IR и NMR спектроскопијом и дифракцијом X-зрака са монокристала. У оба комплекса L^- се координовао тридентатно преко истог сета донорских атома, док је четврто координационо место заузео хлоридни јон. Међутим, комплекси нису изостуктурни због различитих врста нековалентних интермолекуларних интеракција. Ове интеракције су анализиране помоћу Хиршфилдових површина и дводимензионалних графикона отисака прстију.

(Примљено 26. новембра, ревидирано 1. децембра, прихваћено 2. децембра 2020)

REFERENCES

1. P. Heffeter, V. F. S. Pape, É. A. Enyedy, B. K. Keppler, G. Szakacs, C. R. Kowol, *Antioxidants Redox Signal.* **30** (2019) 1062 (http://dx.doi.org/10.1089/ars.2017.7487)
2. J. Shim, N. R. Jyothi, N. A. M. Farook, *Asian J. Chem.* **25** (2013) 5838 (http://dx.doi.org/10.14233/ajchem.2013.oh105)
3. G. Pelosi, *Open Crystallogr. J.* **3** (2010) 16 (http://dx.doi.org/10.2174/1874846501003020016)
4. N. P. Prajapati, H. D. Patel, *Synth. Commun.* **49** (2019) 2767 (http://dx.doi.org/10.1080/00397911.2019.1649432)
5. T. S. Lobana, R. Sharma, G. Bawa, S. Khanna, *Coord. Chem. Rev.* **253** (2009) 977 (http://dx.doi.org/10.1016/j.ccr.2008.07.004)
6. E. J. Siddiqui, I. Azad, A R. Khan, T. Khan, *J. Drug Deliv. Therapeut.* **9** (2019) 689 (http://jddtonline.info/index.php/jddt/article/view/2888/2135)
7. T. R. Todorović, A. Bacchi, N. O. Juranić, D. M. Sladić, G. Pelizzi, T. T. Božić, N. R. Filipović, K. K. Andelković, *Polyhedron* **26** (2007) 3428 (http://dx.doi.org/10.1016/j.poly.2007.03.023)
8. N. Gligorijević, T. Todorović, S. Radulović, D. Sladić, N. Filipović, D. Gođevac, D. Jeremić, K. Anđelković, *Eur. J. Med. Chem.* **44** (2009) 1623 (http://dx.doi.org/10.1016/j.ejmech.2008.07.033)
9. T. R. Todorović, A. Bacchi, D. M. Sladić, N. M. Todorović, T. T. Božić, D. D. Radanović, N. R. Filipović, G. Pelizzi, K. K. Andelković, *Inorg. Chim. Acta* **362** (2009) 3813 (http://dx.doi.org/10.1016/j.ica.2009.04.047)
10. S. Bjelogrlic, T. Todorovic, A. Bacchi, M. Zec, D. Sladic, T. Srdic-Rajic, D. Radanovic, S. Radulovic, G. Pelizzi, K. Andelkovic, *J. Inorg. Biochem.* **104** (2010) 673 (http://dx.doi.org/10.1016/j.jinorgbio.2010.02.009)
11. T. Srdić-Rajić, M. Zec, T. Todorović, K. Anelković, S. Radulović, *Eur. J. Med. Chem.* **46** (2011) 3734 (http://dx.doi.org/10.1016/j.ejmech.2011.05.039)

12. N. Filipović, N. Polović, B. Rašković, S. Misirlić-Denčić, M. Dulović, M. Savić, M. Nikšić, D. Mitić, K. Anđelković, T. Todorović, *Monatsheft. Chem.***145** (2014) 1089 (http://dx.doi.org/10.1007/s00706-014-1197-6)
13. N. R. Filipović, S. Bjelogrlić, A. Marinković, T. Ž. Verbić, I. N. Cvijetić, M. Senćanski, M. Rodić, M. Vujčić, D. Sladić, Z. Striković, T. R. Todorović, C. D. Muller, *RSC Adv.* **5** (2015) 95191 (http://dx.doi.org/10.1039/C5RA19849F)
14. I. S. Djordjevic, J. Vukasinovic, T. R. Todorovic, N. R. Filipovic, M. V. Rodic, A. Lolic, G. Portalone, M. Zlatovic, S. Grubisic, *J. Serb. Chem. Soc.* **82** (2017) 825 (http://dx.doi.org/10.2298/JSC170412062D)
15. S. Poirier, H. Lynn, C. Reber, E. Tailleur, M. Marchivie, P. Guionneau, M. R. Probert, *Inorg. Chem.* **57** (2018) 7713 (http://dx.doi.org/10.1021/acs.inorgchem.8b00724)
16. L. M. Epstein, E. S. Shubina, *Coord. Chem. Rev.* **231** (2002) 165 (http://dx.doi.org/10.1016/S0010-8545(02)00118-2)
17. J. Kozelka, in *Noncovalent Forces*, S. Scheiner, Ed., Springer International Publishing, Cham, 2015, pp. 129 (http://dx.doi.org/10.1007/978-3-319-14163-3_6)
18. P. Ristić, V. Blagojević, G. Janjić, M. Rodić, P. Vulić, M. Donnard, M. Gulea, A. Chylewska, M. Makowski, T. Todorović, T. Todorović, N. Filipović, *Cryst. Growth Des.* **20** (2020) 3018 (http://dx.doi.org/10.1021/acs.cgd.9b01661)
19. P. N. Bourosh, M. D. Revenko, M. Gdaniec, E. F. Stratulat, Y. A. Simonov, *J. Struct. Chem.* **50** (2009) 510 (http://dx.doi.org/10.1007/s10947-009-0078-z)
20. *CrysAlisPro Software system*, Agilent Technologies UK Ltd., Cheadle
21. G. M. Sheldrick, *Acta Crystallogr. Sect. A Found. Adv.* **71** (2015) 3 (http://dx.doi.org/10.1107/S2053273314026370)
22. G. M. Sheldrick, *Acta Crystallogr., C* **71** (2015) 3 (http://dx.doi.org/10.1107/S2053229614024218)
23. C. B. Hübschle, G. M. Sheldrick, B. Dittrich, *J. Appl. Crystallogr.* **44** (2011) 1281 (http://dx.doi.org/10.1107/S0021889811043202)
24. A. L. Spek, *Acta Crystallogr., D* **65** (2009) 148 (http://dx.doi.org/10.1107/S090744490804362X)
25. C. F. Macrae, I. J. Bruno, J. A. Chisholm, P. R. Edgington, P. McCabe, E. Pidcock, L. Rodriguez-Monge, R. Taylor, J. van de Streek, P. A. Wood, *J. Appl. Crystallogr.* **41** (2008) 466 (http://dx.doi.org/10.1107/s0021889807067908)
26. C. F. MacRae, I. Sovago, S. J. Cottrell, P. T. A. Galek, P. McCabe, E. Pidcock, M. Platings, G. P. Shields, J. S. Stevens, M. Towler, P. A. Wood, *J. Appl. Crystallogr.* **53** (2020) 226 (http://dx.doi.org/10.1107/S1600576719014092)
27. C. R. Groom, I. J. Bruno, M. P. Lightfoot, S. C. Ward, *Acta Crystallogr., B* **72** (2016) 171 (http://dx.doi.org/10.1107/S2052520616003954)
28. J. J. McKinnon, D. Jayatilaka, M. A. Spackman, *Chem. Commun.* (2007) 3814 (http://dx.doi.org/10.1039/b704980c)
29. J. J. McKinnon, M. A. Spackman, A. S. Mitchell, *Acta Crystallogr., B* **60** (2004) 627 (http://dx.doi.org/10.1107/S0108768104020300)
30. M. Mohan, M. Manmohan, *Synth. React. Inorg. Met. Chem.* **12** (1982) 761 (http://dx.doi.org/10.1080/00945718208082693)
31. L. Yang, D. R. Powell, R. P. Houser, *Dalton Trans.* (2007) 955 (http://dx.doi.org/10.1039/b617136b)
32. R. Boese, M. T. Kirchner, J. D. Dunitz, G. Filippini, A. Gavezzotti, *Helv. Chim. Acta* **84** (2001) 1561 (http://dx.doi.org/10.1002/1522-2675(20010613)84:6<1561::AID-HLCA1561>3.0.CO;2-M)

33. I. Dance, *New J. Chem.* **27** (2003) 22 (http://dx.doi.org/10.1039/b206867b)
34. M. A. Spackman, J. J. McKinnon, *CrystEngComm* **4** (2002) 378 (http://dx.doi.org/10.1039/b203191b)
35. S. L. Tan, M. M. Jotani, E. R. T. Tiekink, *Acta Crystallogr., E* **75** (2019) 308 (http://dx.doi.org/10.1107/S2056989019001129).